KTH Engineering Sciences

On the influence of surface roughness on rolling contact forces

Oskar Lundberg

Doctoral Thesis

Stockholm, Sweden 2016
The Marcus Wallenberg Laboratory for Sound and Vibration Research
Department of Aeronautical and Vehicle Engineering

Postal address
Royal Institute of Technology
MWL/AVE
SE-100 44 Stockholm
Sweden

Visiting address
Teknikringen 8
Stockholm

Contact
Email: oskarl@kth.se

Akademisk avhandling som med tillstånd av Kungliga Tekniska Högskolan i Stockholm framläggs till offentlig granskning för avläggande av teknologie doktorsexamen måndagen den 7:e november 2016, kl 09:30 i sal F3, Lindstedtsvägen 26, Kungliga Tekniska Högskolan, Stockholm.

TRITA-AVE-2016:75
ISSN-1651-7660
ISBN-978-91-7729-145-9

"Noises are like people.
Once you get to know them, they become friendly."
—from A fine balance by Rohinton Mistry

Abstract

Road vehicle tyres, railway wheels and ball bearings all generate rolling contact forces which are transferred within a finite area of contact between the rolling element and the substrate. Either it is visible or not for the human eye, a certain degree of roughness is always present on the contacting surfaces and it influences the generation of both vertical and lateral contact forces.

The purpose of this investigation is to enhance the understanding and modelling of the influence from small-scale surface roughness on the generation of rolling contact forces. To this end, a computationally efficient method to include roughness-induced contact nonlinearities in the dynamic modelling of rolling contacts is proposed. The method is implemented in a time domain model for vertical wheel–track interaction to model rolling-induced rail vibrations, showing good agreement with measurements. Furthermore, a test rig is developed and used for the investigation of tyre–road rolling contact forces. Detailed studies are performed on the influence of substrate roughness on the resulting contact forces for a tyre tread block which is rolling at different operating conditions. The choice of substrate as well as the rolling velocity and the slip ratio is observed to have significant influence on the resulting friction coefficient. For high slip ratios, stick–slip oscillations appear, exhibiting frequency content which is largely dependent on the choice of substrate. The outcomes of this study can potentially be used to improve future tyre–road contacts with respect to wear, traction and noise generation.

Keywords: Rolling contact, Surface roughness, Contact forces, Contact modelling, Friction, Road, Asphalt, Substrate, Test-rig, Sliding, Stick–slip, Tyre, Rubber, Tread-block, Wheel-rail interaction

Sammanfattning

För alla rullningskontakter, oberoende av om det är fordonsdäck, järnvägshjul eller kullager som avses så överförs alla kontaktkrafter inom ett begränsat område mellan det rullande föremålet och underlaget, kontaktytan. Trots att den inte alltid är synbar för blotta ögat så finns där, både på det rullande föremålet och på underlagets yta, en viss fintextur som påverkar alstringen av såväl de vertikala som de laterala kontaktkrafterna.

Syftet med denna forskning är att utveckla verktyg för modellering av, samt öka förståelsen för hur kontaktytornas fintextur inverkar på de rullningsinducerade krafterna. Som en del av detta, föreslås en beräkningseffektiv metod att inkludera de ickelinjära bidrag som orsakas av ytornas fintextur i dynamiska simuleringar av rullningskontakten. Beräkningsmetoden används för att beräkna de vertikala rälsvibrationer som uppstår i kontakten mellan hjul och räl och resultaten uppvisar god överensstämmelse vid en jämförelse med fältmätningar. Utöver detta har en ny mätrigg utvecklats för att detaljstudera kontakten mellan enskilda däcksmönsterblock och vägbanan. Tydliga skillnader påvisas för de krafter och friktionskoefficienter som uppmätts vid rullning på underlag med inbördes olika fintextur. För höga rullningshastigheter och en högre grad av accelerationsmoment, uppstår tydliga tillstånd av stick-slip-svängningar, vars frekvensinnehåll beror av vilken fintextur underlaget har. Resultaten av denna forskning kan potentiellt användas för att mildra slitage och ljudgenerering i framtida rullningskontakter.

Nyckelord: Rullning, Ytråhet, Fintextur, Kontaktkrafter, Kontaktmodellering, Friktion, Väg, Asfalt, Underlag, Mätrigg, Glidning, Stick–slip, Däck, Gummi, Mönsterblock, Hjul-räl interaktion

Acknowledgments

The Centre for ECO^2 Vehicle Design is gratefully acknowledged for the financial support. Thank you also to Peter, Gunilla, Jenny, Carlos and Susann for the work you have done for us in the Centre!

Ines, thank you for your support, discussions and feedback during the last years. I am extremely grateful for the freedom I have gotten and the confidence you have had in me. Thank you also Svante and Leif for your guidance and feedback. Stefan, Mikael och Anders, thank you for the good collaboration on the papers.

Danilo, för mig är du en förebild, en person jag ser upp till. Tack för ett otroligt bra jobb med mätriggen och alla pratstunder nere i labbet. Uno och Kent, stort tack för det imponerande arbetet med givarna och det trevliga sällskapet i labbet. Tack också till Malin, Monica och Carl vid lättkonstruktioner för möjligheten att mäta glidning och till Johanna, Ingela och Ann-Britt för lunchsällskap och hjälp med olika admin-frågor.

I have met many interesting and kind people during my stay at KTH. I have learned to say some things in Chinese, and then I have forgotten them. Thanks Hao, Chenyang and Lin for trying. I have learned a lot about Persian culture. Thanks for all the laughs, Saeed, Alireza and Matin. Thanks Anna, Elias, Nisse, Karl, Juan, Luck, Anders, Stefan, Romain, Nicolas, Raimo, Emma, Afzal, Rickard, Mohammad, Yubao, Ciarán, Luca, Na Wei, Zhendong, Ulf, Urmas, Leping, and all you other colleagues for good company!

To family (both in Sweden and in Chile) and friends: Thanks for sharing life with me!

Matteo och Alessia, ni är det viktigaste för mig och kommer alltid att vara det. Jag älskar er. Cuánto? Más que infinito!

Carola, gracias por ser quien eres. Nunca me aburro contigo. Sabes cómo disfrutar de la vida y yo quiero estar allí contigo, disfrutandola.

Resarö, October 11, 2016

Papers included in the Doctoral thesis

This thesis consists of a summary and the following papers:

A O.E. Lundberg, S. Finnveden, S. Björklund, M. Pärssinen and I. Lopez Arteaga. A nonlinear state-dependent model for vibrations excited by roughness in rolling contacts. *Journal of Sound and Vibration* 2015; 345, pp. 197-213.

B O.E. Lundberg, A. Nordborg and I. Lopez Arteaga. The influence of surface roughness on the contact stiffness and the contact filter effect in nonlinear wheel–track interaction. *Journal of Sound and Vibration* 2016; 366, pp. 429-446.

C O.E. Lundberg, I. Lopez Arteaga and L. Kari. A compact internal drum test rig for measurements of rolling contact forces between a single tread block and a substrate. *Submitted to Measurement* 2016.

D O.E. Lundberg, L. Kari and I. Lopez Arteaga. Friction of a rubber tread block in rolling and sliding contact with asphalt—An experimental study. *Submitted to Wear* 2016.

E O.E. Lundberg, L. Kari and I. Lopez Arteaga. An experimental study on the influence of substrate roughness on the friction of a tread block in rolling and sliding contact. *To be submitted* 2016.

Division of work between the authors of the papers

A Lundberg developed the theory and wrote the paper. Björklund provided the boundary element contact model and Pärssinen provided the measurement results. Finnveden and Lopez Arteaga discussed the theory and supervised the work.

B Lundberg performed the analysis and wrote the paper. Nordborg provided the wheel–rail dynamic interaction model (rwc) and discussed the analysis. Lopez Arteaga supervised the work.

C Lundberg developed the test-rig and wrote the paper. Lopez Arteaga and Kari supervised the work.

D Lundberg performed the measurements and the analysis and wrote the paper. Lopez Arteaga and Kari supervised the work.

E Lundberg performed the measurements and the analysis and wrote the paper. Lopez Arteaga and Kari supervised the work.

Contents

Part I

Overview and Summary

Chapter 1

Introduction

1.1 Motivation and background

The first scholar record of a distinction between rolling friction and sliding friction dates back to Leonardo Da Vinci (1452–1519) who even invented a ball bearing as a part of his helicopter-design. Although the helicopter was never even close to take off, the use of a rolling contact bearing must have taken him closer to his goal. Some three to four hundred years later, railway systems, engine driven road vehicles and machines relying on rolling elements in bearings and gears where developed. Today, rolling is found in for instance laptops which are cooled with fans using ball bearings and in the astonishing amount of global transports conveyed by rolling. In fact, vehicles rolling on railway wheels, passenger car tyres and truck tyres together account for approximately 75 % of the oil consumption used globally for transportation [14]. As a consequence of the vast amount of rolling contacts present in today's society, their efficiency, durability and degree of noise generation have a large impact on the society as a whole. Therefore, there is great potential in any design improvement which leads to a more environmentally friendly and less noisy rolling contact.

The main reason to make use of rolling contacts in different applications is their inherent low resistance to motion. In fact, if pure rolling is considered, there is no resistance to motion whatsoever and the contact area is reduced to a single point (if we assume the rolling element to be a ball). Naturally, a point contact can never exist in reality since it requires the use of infinitely stiff materials. But in some ball bearings in which high quality steel is used and the contact surfaces are extremely smooth, the near absence of hysteretic losses lead to very low resistance to motion. As the degree of material deformation is very low, so is the contact area within which lateral forces can be transferred between the rolling element and the substrate. In

ball bearings, this lack of a sufficiently large contact area, a cage, an inner ring an and outer ring are used to guide the rolling elements.

Although the use of high quality steel in rolling contacts leads to small deformations, there is still a finite upper limit for its rigidity. As the normal load increases, so will the material deformation and hence also the contact area. An example of this situation is the contact between the railway wheel and the rail. The weight of a typical passenger train induces normal contact forces of approximately 60 kN on each wheel–rail contact which in turn leads to a normal deformation of roughly $75\,\mu$m and a contact patch size of approximately $1\,\text{cm}^2$. The creation of this contact area is of utmost importance since it provides an extended area on which friction mechanisms can operate and enable traction and braking forces for railway vehicles. However, due to the smooth steel surfaces and the small contact area, friction mechanisms are rather weak, leading to long acceleration and braking distances. This may have a negative impact on transportation systems such as the metro of Santiago de Chile (roughly 2.5 M passengers daily) where long acceleration and braking distances prevent the desired high transportation efficiency. As a countermeasure, acceleration and braking distances are there reduced by replacing the steel wheels by pneumatic tyres for which effective friction mechanisms and a large contact patch lead to drastically increased available friction. A more common use of pneumatic tyres is of course in road and off-road vehicles which possess very good traction, braking and steering manoeuvrability. However, compared to steel–steel rolling contacts, both the Santiago metro system as well as road and off-road vehicles suffer the consequences of increased rolling resistance due to hysteretic losses. A trade of between a low rolling resistance and a high vehicle manoeuvrability thus apply for all transports conveyed by rolling, as is presented in Fig. 1.1.

To successfully investigate the effects of this trade-off and other important aspects of rolling contacts, it is key to understand the generation of forces during rolling as well as the resulting vibratory deformations in both the rolling element and the substrate. The vibratory deformations lead to undesired effects such as the already mentioned rolling resistance, sound radiation, durability (wear) and possibly comfort vibration issues. The understanding and modelling of the vibratory deformations are therefore important research tasks which are well advanced [6]. However, when it comes to the modelling and understanding of the contact force, which is in fact the source of the vibratory deformations and the direct reason why traction, braking and wear of contact materials exist, there are yet some challenges which demand future research. This thesis embraces one of these challenges which is the influence of surface roughness on the generation of rolling contact forces. Independent of the application at hand, all rolling

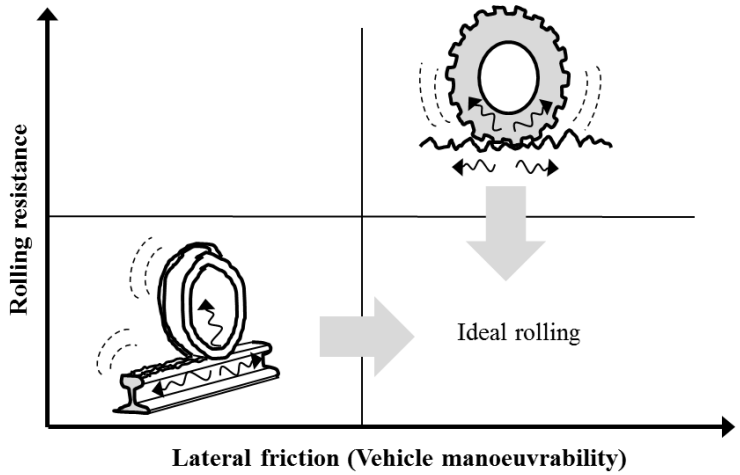

Figure 1.1: Trade off between low rolling resistance and high vehicle manoeuvrability (available friction).

contact forces (vertical and lateral) are transferred within a finite area of contact between the rolling element and the substrate. Zooming in at this area of contact, also called the contact patch, we will observe that it is in fact built up by islands of contact within the larger area of contact. This might be rather intuitive when thinking of a tyre rolling on asphalt, but it is not equally clear for the contact between nominally smooth surfaces such as those of railway wheels and rails. However, either it is visible or not for the human eye, a certain degree of roughness on the surfaces in rolling contacts is always present, and its influence on the generation of both vertical and tangential contact forces must be further investigated.

1.2 Problem definition and solution approach

The goal for this thesis is to increase the understanding and improve the modelling capabilities for the influence from small scale surface roughness on the resulting rolling contact forces. This, to facilitate the design of more environmentally friendly, less noisy and more predictable rolling contacts.

In metal–metal rolling contacts, a consequence of the relatively small areas of contact is that only small errors are introduced if the force is assumed to act in a point instead of being distributed over a contact patch. Although this simplification enables a highly efficient modelling of the forces which arise in the rolling contact, the accuracy of predictions still relies on a suitable description of the relation between the resultant force magnitude and the material deformation in the point of contact. Considering only perfectly smooth surfaces, most engineering metal–metal rolling contacts are well described by Hertz' theory of contact, which includes analytical descriptions

of the relation between force and deformation for contacts which have circular and elliptical areas of contact. However, the contact surfaces in real contact conditions exhibit a certain degree of small scale roughness which is characterised by wavelengths in the order of or shorter than the typical dimensions of the contact patch. This small scale roughness may influence the relation between vertical contact force and deformation and what more, the dynamic excitation related to such small scale roughness is known to be heavily reduced, introducing spatial contact filtering. Unfortunately, Hertz' theory is unable to account for these two effects related to the small scale roughness of the contacting bodies. Since the effects may be significant for the resulting rolling contact analysis at hand, detailed boundary element methods and finite element methods are sometimes used to model the contact forces. This is however avoided and sometimes not even feasible due to the drastically increased requirements of input roughness data and the largely increased computational cost. There is therefore a need for computationally efficient modelling procedures which include the effects of small scale roughness in the dynamic interaction of metal–metal rolling contacts.

A computationally efficient way to include the influence from small scale roughness is to pre-calculate the relation between force and deformation as well as that of spatial contact filtering, using boundary element computations including measured or synthesised small scale roughness. These relations are subsequently included in a point force expression which is used in time domain modelling of the dynamic interaction in metal–metal rolling contacts.

The relatively low rigidity of rubber (in contrast to that of metal) leads to large material deformations in the tyre–road rolling contact. This, together with the viscoelastic character of rubber and the typically higher degree of surface roughness on roads compared to that of metal–metal contacts leads to some fundamental differences between these rolling contact conditions. The inventor of the pneumatic tyre, Robert Thomson, explicitly claimed that "diminishing the noise they make when in motion" was one of the main features of his invention from 1847 [30]. In addition to this feature, the pneumatic tyre owes its success mainly to (1) its ability to transfer very high longitudinal and transverse forces between the vehicle and the road and (2) its ability to effectively mitigate the normal contact forces which originate in the impact of the tyre tread against road surface irregularities. These qualities deliver good handling, safety and comfort for road vehicles despite the sometimes very high vehicle speeds. However, the increased demand and widespread presence of road vehicles in society also expose the adverse effects associated with the pneumatic tyre. Decreased rolling resistance, mitigation of interior and exterior noise as well as tyre wear are therefore increasingly important topics for the vehicle industry and research institutes

worldwide. These undesired effects all have their origin in the generation of forces within the contact patch as is schematically shown in Fig. 1.2.

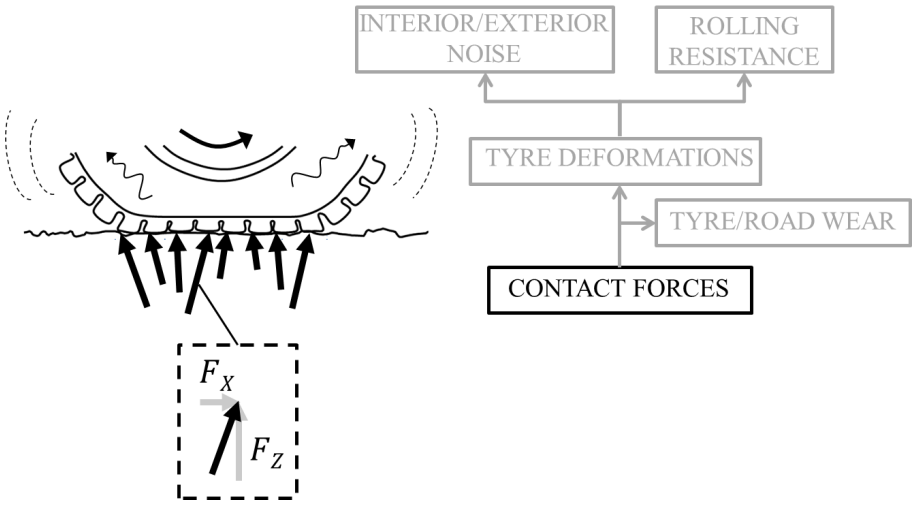

Figure 1.2: Contact forces in the tyre–road interface generate interior and exterior noise as well as rolling resistance and wear. The transverse force component is left out in this two dimensional sketch.

In general, an increased modelling accuracy and enhanced physical understanding have been gained for all aspects presented in Fig. 1.2 during the last decades [19, 6, 4, 27]. However, higher demands on vehicle systems to be environmentally friendly, safe and comfortable indicate a further need for research of underlying physical mechanisms as well as the modelling of these. One identified uncertainty concerns the influence of the longitudinal contact force component on the excitation of tyre vibrations. This uncertainty is partly due to the lack of a complete physical description of the generation mechanisms of tyre–road friction forces. Moreover, the high computational effort required to model the details of friction force generation is further limiting the development of reliable physically based modelling. Conclusively, an important challenge remains to increase the understanding and to find computationally efficient, yet sufficiently detailed models which describe the longitudinal force generation at relevant operating conditions and for arbitrary road surface substrates.

Experimental investigations are effective to increase the understanding of the friction force generation and possibly, they can lead to valuable input to modelling based research. A test rig for rolling contact between a single tyre tread block and a substrate can be specially designed to enable detailed three-axial force measurements close to the contact. The experiment can be designed for typical operating conditions (velocity, acceleration, braking, normal load), but excluding the influence from the tyre structure, focusing primarily on the interfacial rubber–substrate contact details.

1.3 Contributions

The contributions of this thesis are presented as a whole in Part II, in the form of appended papers. Paper A presents a computationally efficient method to include the influence of small scale roughness in the modelling of metal–metal rolling contacts. The method is subsequently adapted and implemented for a wheel–rail rolling contact. The results from this implementation are presented in Paper B together with a comparison to field measurements. Paper C, D and E discuss experimental investigations of the force generation in the tyre–road contact. In Paper C, the design and use of a novel test rig is presented. The test rig is used to accurately measure the contact force of a single tyre tread block in rolling contact with a substrate. In Paper D, the presented test rig is used to perform parametric analyses of the influence of rolling velocity and traction on the force histories for individual tread block passages along the length of the contact patch. In addition, experimental dynamic elastic characterisation of tread block sample as well as of the frictional characteristics of sliding between the sample tread block and the sample substrate are presented. Finally, using the test rig presented in Paper C, a study of the influence of different substrates on the resulting rolling contact forces and corresponding friction coefficients is presented in Paper E. A more comprehensive summary of the contributions are found in Ch. 4, wherein each of the appended papers is summarised.

1.4 Thesis outline

This thesis is organised in two parts; Part I includes an introduction, some background theory and a short summary of the contributions. Part II contains the full contribution of this thesis in the form of appended papers.

Part I starts with an introduction, which is followed by background theory of contact mechanics and the influence from surface roughness on the interfacial force generation in rolling contacts. Metal–metal rolling contacts are introduced in Ch. 2, wherein the generation and modelling of vertical contact forces are discussed. In the subsequent chapter (Ch. 3), tyre–road rolling contact is reviewed with emphasis on the longitudinal component of the contact force and the characterisation of interfacial friction. The contributions of this thesis are summarised in Ch. 4, where each of the appended papers is briefly presented. Finally, Part I ends with some concluding remarks in Ch. 5 and suggestions for future work in Ch. 6.

Chapter 2

Vertical excitation in metal–metal rolling contacts

2.1 Influence of surface roughness

In metal–metal rolling contacts, smoother surfaces are in general preferred to rough surfaces, since they lead to less noise and vibration, less wear and less rolling resistance. However, the material characteristics and the manufacturing process sets a lower limit for the surface roughness. Either the surface is more or less rough, it will in any case lead to a texture-dependent dynamic excitation of contact forces which is determined by the amplitude and wavelength of the surface texture. A general relation between surface texture wavelength and vibration-related aspects in rolling contacts is shown in Fig. 2.1.

In the rolling contact, a time-dependent rolling contact force F_{r} is generated on the rolling object and on the substrate. The contact patch formed in metal–metal contacts is (due to the high rigidity) very small and the contact can therefore, from a structural dynamics point of view, be approximated by a moving point force[1]. This approximation leads to computational efficiency for the modelling of rolling contacts, but as is further discussed in Sec. 2.1.1, it also ignores the effects of surface texture wavelengths which are shorter than the contact dimensions.

Assuming the rolling speed v_{r} to be constant leads to a linear relation between the position of a moving point force and time

[1] From a structural dynamics point of view, this assumption is valid as long as the contact area is small compared to the dynamic wavelength of the excited structures at all frequencies of interest. In other words, wave propagation within the contact area is assumed to have negligible influence on the resulting dynamics.

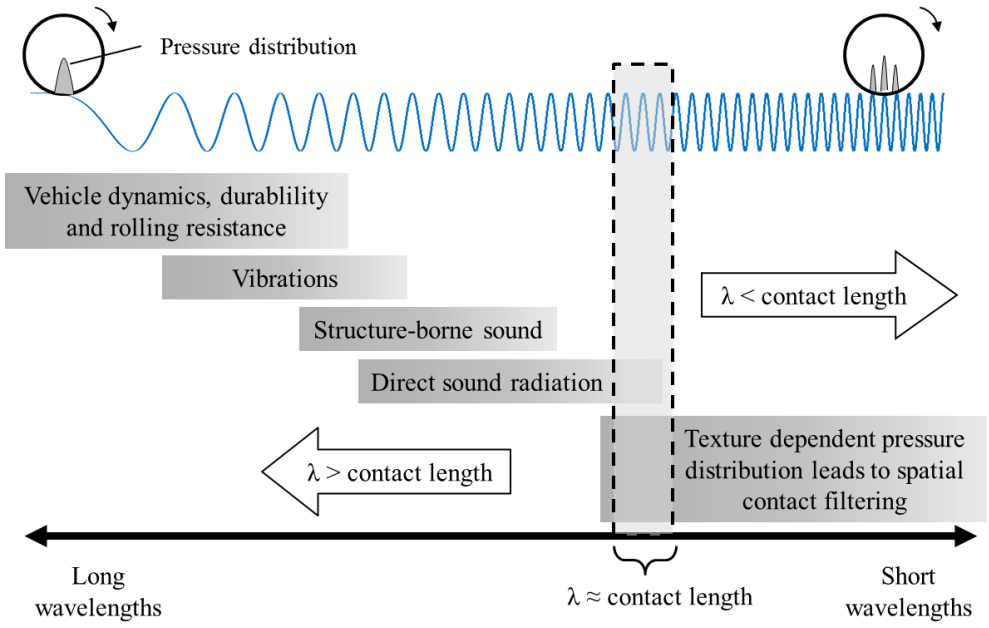

Figure 2.1: Relation between surface texture wavelength and vibroacoustic aspects caused by rolling excitation.

$$F_{\mathrm{r}}(x,t) = F_{\mathrm{c}}\,\delta(x - v_{\mathrm{r}}t)\ . \tag{2.1}$$

If the surface texture of the rolling element or the substrate has a waviness with a wavelength λ which is longer than the dimensions of the contact patch (see Fig. 2.3), it follows from Eq. (2.1) that a force with the frequency

$$f = \frac{v_{\mathrm{r}}}{\lambda}\ [Hz]\ , \tag{2.2}$$

will excite both the rolling element and the substrate. This relation is essential for the understanding of the dynamic response to rolling excitation, since the rolling contact in general takes part of complex coupled systems where the excitation of structural resonances often lead to negative effects as is schematically shown in Fig. 2.1. Very long wavelengths lead to low frequency excitation which—in case of coincidence with structural resonances—might lead to structural durability problems and high rolling resistance. For shorter wavelengths, comfort-related aspects such as vibrational disturbance and structure borne sound problems may appear. Even shorter wavelengths are usually accompanied by direct sound radiation from the rolling object or the supporting structure.

2.1.1 Influence of wavelengths which are shorter than the contact dimensions

For wavelengths which are as short as or even shorter than the dimensions of the contact patch, a spatial dynamic contact filtering is activated. The dynamic excitation which for longer wavelengths follows the relation in Eq. (2.2) starts to break down (see Fig. 2.3). The analogy with boats and ships serve to clarify the effect of dynamic contact filtering, see Fig. 2.2. Since the vessels are of different sizes, so are the contact lengths and therefore they will respond differently to the same ocean wave excitation.

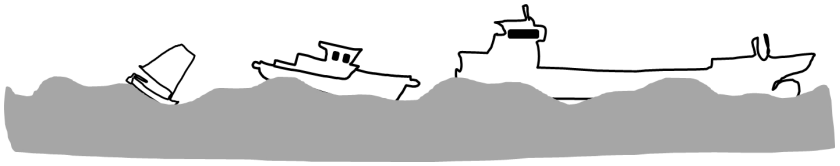

Figure 2.2: Because of the short contact length of the dinghy, it is affected even by the shortest wavelengths. The larger towboat is affected only by the longer wavelengths whereas the freight ship is not affected by any of the ocean wavelengths.

This effect can in frequency domain be thought of as a mechanical low pass filter where the dynamic excitation from contact forces caused by roughness wavelengths shorter than the contact patch is effectively reduced. The surface texture wavelengths which are subject to contact filtering varies greatly between the different rolling contact applications since the size of the contact patch depend on material elasticity, shape of the contacting bodies as well as the applied normal load.

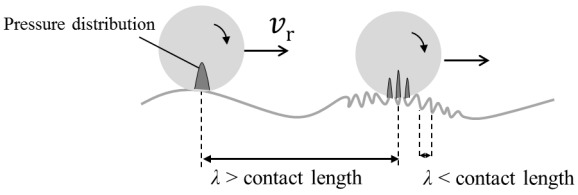

Figure 2.3: Surface roughness excitation for wavelengths which are longer than the contact dimensions and shorter than the contact dimensions.

In addition to the spatial filtering effect, the roughness wavelengths shorter than the contact dimensions are observed to alter the nonlinear relation between force and relative displacement. The resulting contact force due to a normal relative displacement r between the rolling element and the substrate is determined by integrating the contact pressure p over the contact area A. Since the magnitude and distribution of contact pressure within the contact patch depends on the surface texture, so does the resulting contact force

(see Fig. 2.4). As a consequence of this, the relation between the force and the relative displacement is nonlinear not only due to the shape of contacting bodies, but also due to the surface texture within the contact area.

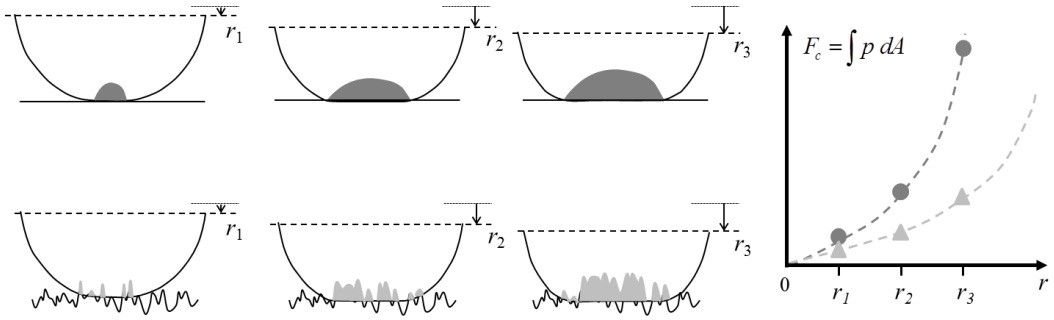

Figure 2.4: The pressure magnitude and distribution within the contact patch depend on surface texture, which in turn leads to an influence on the relation between force and relative displacement between rolling element and substrate.

2.2 Modelling of vertical contact force

The excitation of vibrations resulting from rolling is, as previously discussed in this chapter, the root cause of several negative effects which can be qualitatively separated into different ranges of excitation frequencies (see Fig. 2.1). The excitation frequency due to rolling depends on the rolling velocity as well as the surface texture wavelength as shown in Eq. (2.2). However, in order to quantify the effect of the excitation, the magnitude of the rolling contact force is sought for each position along the rolling path. Assuming that the material properties are known and that the shape of the contact patch is either circular or elliptical, an analytical solution for this was found by Heinrich Hertz already in 1880 [13]. During his Christmas vacation, Hertz, who at the time was a PhD-student, was studying two glass lenses and the optical interference fringes emerging in the gap between them. He noticed that the contact pressure between the lenses lead to elastic deformation which influenced the optical interference. This discovery triggered Hertz to develop a theory for the stresses resulting at the contact of two elastic solids [15]. As a result, he had laid the foundation of the field of contact mechanics and developed a theory which is still used to model metal–metal contacts such as that of the wheel–rail contact and the contact in rolling element bearings[2]. The contact theory of Hertz is an elegant analytical

[2]Heinrich Hertz continued his research on a different topic and in 1888 he published his discovery of electromagnetic waves. When asked by one of his students about the possible use of the discovery which eventually lead to innovations such as the telegraph, radio transmitters and television he replied: "*It's of no use whatsoever. This is just an experiment that proves Maestro Maxwell was right.*" [1]

solution which relates the relative displacement to a pressure distribution within the contact patch. Hence, it offers a computationally efficient and in many cases sufficiently accurate model to predict the rolling contact forces in dynamic coupled systems. However, the assumption of perfectly smooth surfaces as well as the limitation to perfectly circular or elliptical contact areas makes the theory inadequate for studies on the influence of surface roughness. In order to include the effect of surface roughness on nominally flat surfaces, Greenwood and Williamson [9] presented a theory which is based on statistical measures of the surface roughness. Although it is still computationally efficient, the theory of Greenwood and Williamson is not capable of finding the exact pressure distribution for a specific contact condition. Thus, for detailed studies on the influence of surface texture on the resultant pressure distribution and, eventually on the dynamic excitation in rolling contacts, a numerical boundary element model implemented by Björklund [2] is presented below and is further being used for the work presented in Paper A [21] and Paper B [24].

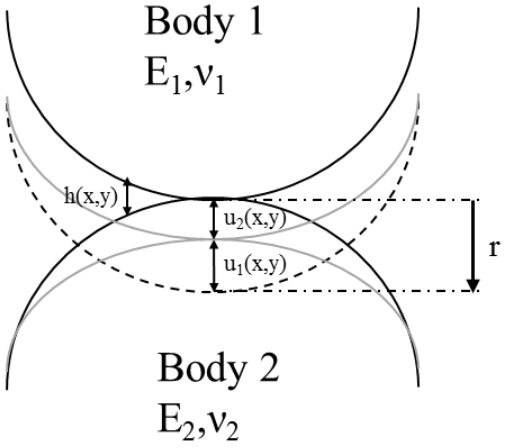

Figure 2.5: Schematic figure of body 1 pressed into body 2. Black lines shows undeformed bodies and gray lines show deformed bodies.

The goal of the performed contact simulations is to relate a known relative displacement to a sought pressure distribution inside the contact area. With reference to Fig. 2.5, the boundary conditions for the contact theory are

$$u_1(x,y) + u_2(x,y) + h(x,y) \left\{ \begin{array}{ll} = r & \text{inside contact area} \\ > r & \text{outside contact area} \end{array} \right\} , \qquad (2.3)$$

relating the relative displacement between the contacting bodies, r to the deformation of body 1, $u_1(x,y)$ and body 2, $u_2(x,y)$ as well as the gap between the contacting bodies before deformation, $h(x,y)$.

Assuming infinite half-space behaviour, an expression for the deformation under a static point load

$$u_z(r) = \frac{1-\nu^2}{\pi E}\frac{P}{l}, \tag{2.4}$$

was first derived in the used form by Boussinesq in 1885 [3]. Here, E is the elastic modulus and ν is Poissons ratio while P is the point load and l is the distance from the point load. In Fig. 2.4, an example of unit deformation and the resulting pressure distribution calculated using Eq. (2.4) is shown.

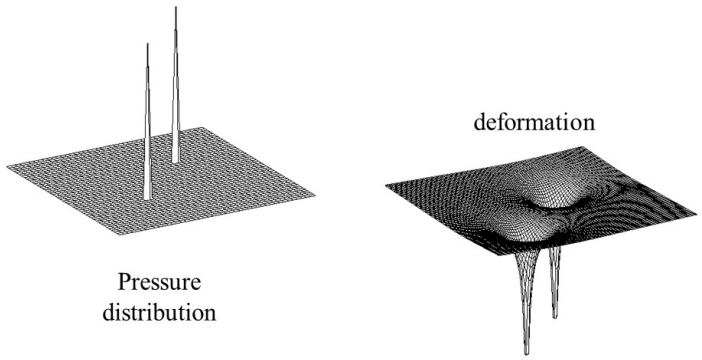

Figure 2.6: Example of unit deformations in two points and the corresponding pressure distribution calculated with Eq. (2.4).

Expanding this theory from a point to a contact region leads to a more general expression for the deformation at any point (x, y) due to a sum of the forces acting in all other points (ξ, η) within the contact region [15],

$$u_z(x,y) = \iint_S \frac{1-\nu^2}{\pi E}\frac{p(\xi,\eta)}{\sqrt{(x-\xi)^2+(y-\eta)^2}}\,d\xi\,d\eta\ . \tag{2.5}$$

Here, instead of a point force, the force is acting over a small rectangular area $d\xi d\eta$ which has its center point at (ξ, η). By combining Eq. (2.5) with the boundary conditions for a normally loaded contact in Eq. (2.3) an expression for the equilibrium between two objects in contact is found

$$\frac{1}{\pi E_*}\iint_S \frac{p(\xi,\eta)}{\sqrt{(x-\xi)^2+(y-\eta)^2}}\,d\xi\,d\eta \left\{ \begin{array}{ll} = r - h(x,y) & \text{inside contact area} \\ > r - h(x,y) & \text{outside contact area} \end{array} \right\}, \tag{2.6}$$

where

$$\frac{1}{E_*} = \frac{1-\nu_1^2}{E_1} + \frac{1-\nu_2^2}{E_2}. \tag{2.7}$$

Making use of Eq. (2.6), the deformation in any point (x, y) due to a pressure distribution $p(\xi, \eta)$ can be calculated. Reciprocally, the pressure distribution can be calculated if the distribution of deformations in the contact area is known. On beforehand, the area of contact is unknown and must therefore be guessed initially. An iterative process then leads to the correct contact area as the grid cells found outside the contact area are removed from the solution. Identification of the cells which are not in contact is achieved by the inequality in the second row of Eq. (2.6). The expression in Eq. (2.6) is rewritten on matrix form which enables an efficient computational procedure,

$$\mathbf{Cp} = (r - \mathbf{h}), \tag{2.8}$$

forming a pure elastic contact model. Here, the matrix **C** contains discretised versions of influence coefficients $C_{i,j}$, relating the deformation in cell i to the pressure in cell j for all i, j when $i \neq j$. The pressures for all cells inside the contact area are found in the array **p**. The relative displacement between the rolling element and the substrate is found in the scalar *r*. The array **h** contains the gap between the contacting partners for each cell before deformation, i.e. when the bodies are brought together but no deformation has yet occurred. Contact simulations are here limited to normal displacements, although both normal and tangential displacements are present for real dynamic contacts. Furthermore, both the rolling element and the substrate are assumed to act as infinite half spaces in the contact region. To conclude, the total normal force F_c, due to a specified relative displacement is found by numerical integration of the pressures over the total contact area,

$$F_c = \sum \mathbf{p} S, \tag{2.9}$$

wherein S is the grid cell area.

Chapter 3

Longitudinal forces in tyre–road rolling contacts

A tyre which is mounted on a vehicle and is rotating freely around its own axis does not lead to any linear motion for the vehicle until it is set into contact with a substrate. If the interfacial friction between the tyre and the substrate is sufficient, longitudinal contact forces are generated and a linear motion is exerted on the tyre centre point, and thus also on the whole vehicle. In this chapter, the generation of longitudinal contact forces F_x is discussed by the study of a single tyre tread block and its motion through the contact patch.

The tread block undergoes a rotary motion until it approaches the contact patch where the vehicle loading causes the tread to bend and compress. This leads to a transition from rotary motion to a linear motion and is part of the impact phase. Subsequently, the tread block enters the contact phase, where it is compressed and subject to linear motion through the centre part of the contact length. Finally, the trailing edge is approached and the tread block enters the release phase where a reversal bending and a decompression take place, leading to a reversed transition from linear motion to a rotary motion. The bending and compression of the tyre when it goes through the contact patch give rise to longitudinal forces on the tread block which in the impact phase act in the tyre rolling direction and in the release phase act in the direction of the vehicle. For perfectly free rolling tyres, these contributions balance each other and lead to a zero net longitudinal force. However, in all real rolling conditions there is always a net longitudinal acceleration or braking present in the tread block–road contact although it can be low in magnitude if it is present only to overcome the rolling resistance of the vehicle. The mechanisms behind the generation of this longitudinal force are observed to produce a difference between the tyre velocity v_{t} and the vehicle velocity v_{v} as schematically depicted in Fig. 3.1. This difference in velocity is

named the slip velocity and after being normalised with the vehicle velocity, it is defined as the slip ratio [7]

$$s_x = \frac{v_\mathrm{t} - v_\mathrm{v}}{v_\mathrm{v}} \,. \tag{3.1}$$

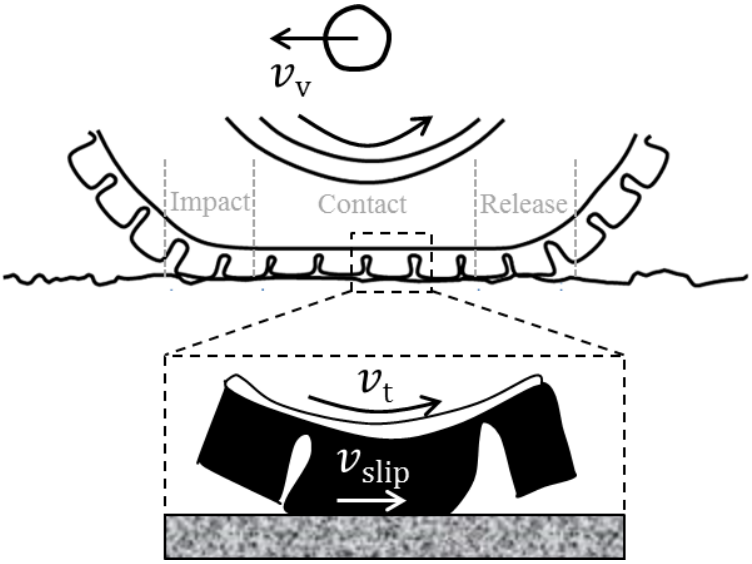

Figure 3.1: Schematic figure of the path of a tread block through the contact patch where a slip velocity between the tread block and the road exist (partly adapted from [12]).

The slip ratio takes positive values for acceleration and negative values for braking. Typically, the potential of a certain contact condition to transmit longitudinal forces is characterised by the longitudinal friction coefficient

$$\mu_x = \frac{F_x}{F_z} \,, \tag{3.2}$$

where F_z is the vertical contact force component. The coefficient of friction for the tyre–road contact depend on many parameters such as the tyre dimensions, rubber compound and inflation pressure, the road surface texture and humidity, the rolling velocity, the temperature and the normal load. The coefficient of friction for a specific combination of operating and contact conditions is frequently presented as a function of the slip ratio [8]. An example of such relation for a tyre rolling on a dry road surface is presented in Fig. 3.2. The underlying mechanisms for the slip which are observed to coincide with the generation of longitudinal contact forces may be elastic deformation of the tyre tread as well as sliding within the contact patch or, more likely due to a combination of these [11]. The slip mechanisms for a dry tyre–road contact can be understood by a simplified separation into the regions A, B and C in Fig 3.2.

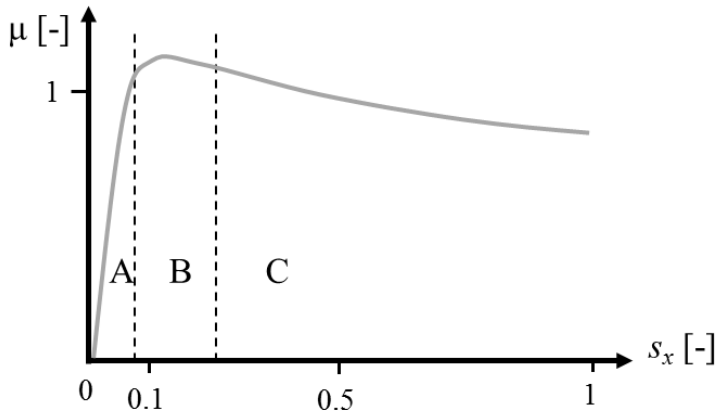

Figure 3.2: Friction coefficient as a function of slip ratio between a tyre and a dry road (adapted from Xie [32]).

Region A correspond to cruising and moderate acceleration or braking for which the friction is mainly caused by tread rubber elastic deformation and the slope of the friction curve therefore reflects the longitudinal stiffness. High acceleration or braking leads to slip ratios within region B, where a transition from predominant rubber elastic deformation to gross sliding within the contact patch occurs. A maximum value for the friction coefficient is usually found in this region. Vehicle traction and braking control systems are therefore tuned to maintain the slip ratio within the range of region B. Heavier acceleration or braking lead to slip ratios within region C, where the coefficient of friction is expected to decrease. The slip is here predominantly due to gross sliding between tread and road and the friction coefficient reaches its asymptotic value for slip ratios $s_x \gg 0.1$ [8].

3.1 Dynamic properties of tread rubber

Although the deformation slip and sliding between the tread block and the substrate are observed to generate longitudinal forces, it is at this point of the analysis not clear how this occur. In order to clarify this, a review of the dynamic properties of rubber is required. It is identified that the processes which influence the interfacial friction are present both within the tread rubber itself as well as in the interfacial details of the contact patch [10, 26]. Tyre tread rubber is a viscoelastic material which means that it is deformable with a behaviour which lies between that of a viscous liquid and an elastic solid. In essence, this means that the energy used to deform the rubber is partly recovered and partly converted into heat, introducing mechanical losses. Moreover, the long entangled polymer chains lead to a frequency dependence for the rubber dynamic properties. The inclusion of reinforcing

fillers (such as carbon black or silica) and the vulcanisation process, where sulfur bridges are formed between polymer chains, drastically increases the strength of the rubber and makes it more brittle elastic. Although the reinforcing fillers introduce a nonlinearity in the dynamic properties of the rubber with respect to deformation amplitude, it has been shown that a linear viscoelastic model of the tread rubber can lead to satisfactory predictions of the tyre tread dynamics [18]. The principal character of the frequency dependence of the tread rubber elasticity and the energy losses is shown in Fig. 3.3.

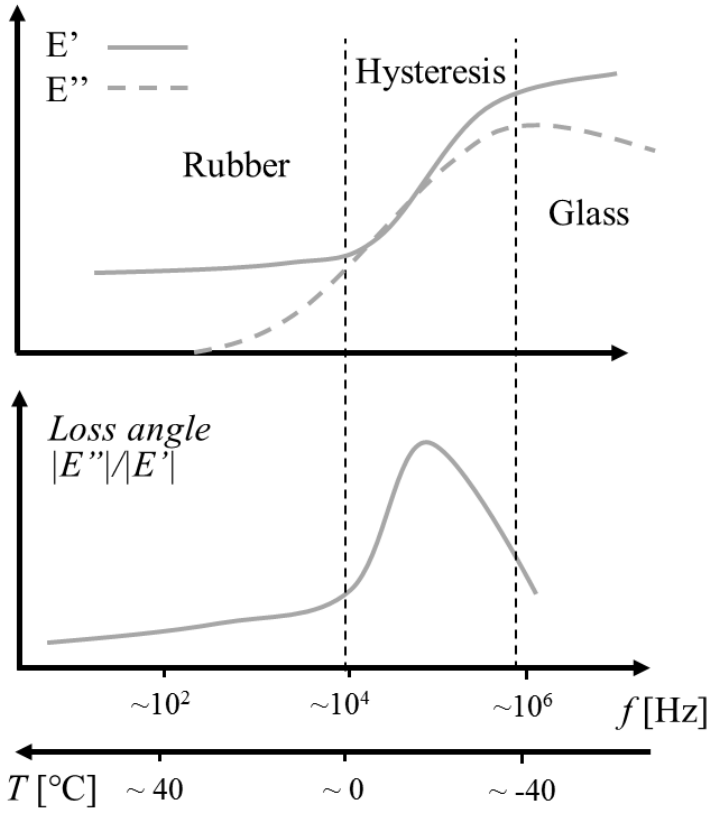

Figure 3.3: Top: Principle character of a tread rubber storage modulus (solid line) and loss modulus (dashed line) of elasticity and bottom: principle character of the corresponding loss angle as a function of excitation frequency or temperature [5]. A schematic separation into a rubbery, hysteresis and glassy region.

The dynamic characteristics can be separated into a soft elasticity (or rubbery) region, a hysteresis region and a brittle elasticity (or glassy) region. The excitation frequency and the temperature has been observed to have a reversed effect on the rubber dynamic properties [10]. A low temperature thus implies a brittle elasticity as in the glassy region whereas a high temperature correspond to the rubbery region, where the rubber has a soft elasticity. The hysteresis region correspond to intermediate temperatures for

which maximum mechanical losses occur. Since the temperature has nearly the opposite effect on the rubber dynamics as that of the frequency, it is common to experimentally characterise the dynamic properties of rubber for a wide range of temperatures instead of for a very wide range of frequencies [26]. A shift factor can thus be defined to shift the modulus of elasticity horizontally along the frequency axis using only measurement data obtained at different temperatures. It is observed that the rubber dynamic properties which lies within the hysteresis region in Fig. 3.3 is of great importance for both the dominant contributions to the generation of longitudinal forces: adhesion and hysteresis, which are both discussed below. Other, less contributing mechanisms are mentioned in the literature, such as the cohesive friction, which is due to tearing of the molecular chains and the viscous friction, which appear in a layer of viscous material such as water in between the rubber and the substrate [16]. These contributions are in general much lower than those from adhesion and hysteresis and are not further discussed in this thesis.

3.2 Fundamental mechanisms of tyre–road friction

Adhesive friction is formed by the sum of molecular attraction (such as Van der Waals bonds) in the rubber–substrate interface. If there is sliding between the rubber and the substrate and a molecular bond has been formed, it is subsequently stretched, resulting in a frictional force which peaks when the bond brakes. Finally a new bond is formed which completes a cycle of the repetitive formation, stretching and braking of bonds. The longitudinal force generated in this manner depend on very close contact since bonds are formed on a molecular scale [31] and consequently, adhesive friction is higher for smooth contacts than for rough contacts. Moreover, the adhesive force depends on the sliding velocity between the rubber and the substrate, where the longitudinal force is maximised if the ratio between the length of a fully stretched molecular bond and the time it takes to form, brake and reform the molecular bond is similar to the sliding velocity [29, 31]. For tread rubber, this relation leads to excitation of molecular adhesion in the approximate frequency range of 10^5–10^8 Hz for a constant temperature of approximately 20°C. The resultant longitudinal force due to adhesion is generally modelled as the real area of contact times the shear stress caused by the sum of all attractive bonds within the same real area of contact [25]

$$F_{x,\mathrm{a}} = \tau_x(v_{\mathrm{sl}})A(v_{\mathrm{sl}}, C) \ . \tag{3.3}$$

Therein, the real area of contact A depends on both the sliding velocity v_{sl} and the surface roughness, which is here represented by its power spectral density $C(q)$ as a function of the wavenumber. The shear stress τ_x also depends on the sliding velocity since it exhibits a maximum when the ratio between the sliding velocity and a length on molecular scale equals the maximum of the rubber loss angle.

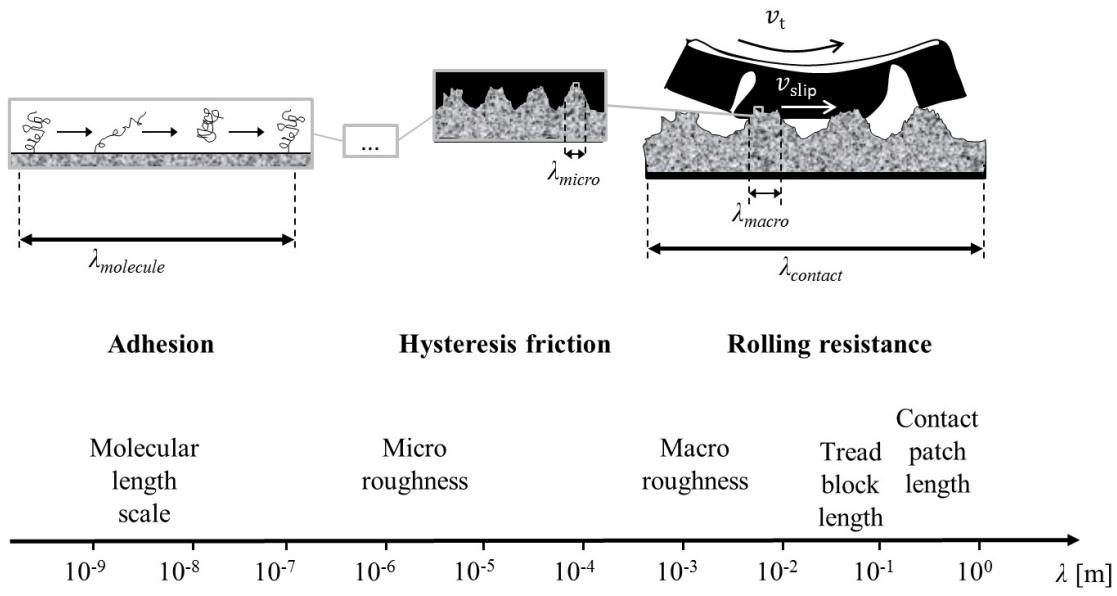

Figure 3.4: Schematic figure of the different length scales which influence the generation of the longitudinal forces in the tyre–road contact.

The hysteresis friction component originates in the deformation of tread rubber around asperities of the road surface. When the rubber slides longitudinally and impacts the front of an asperity it will due to its elasticity deform, which result in a vertical as well as a longitudinal force component. However, the viscosity of the rubber prevents an immediate return to its initial undeformed state as it has reached the back of the asperity. The force component which was generated on the front of the asperity is therefore not fully balanced by that of the back, hence generating a net longitudinal friction force. The magnitude of the resultant longitudinal force which is due to hysteresis friction thus depends on the surface roughness amplitude and wavelength, the sliding velocity and the rubber viscoelastic bulk properties. A computationally efficient procedure to model the hysteresis friction coefficient which couples a broad range of surface roughness wavelengths to the viscoelastic properties of rubber is proposed by Persson [28] as well as by Heinrich and Klüppel [12] who described the resultant longitudinal force due to hysteresis as

$$F_{x,\mathrm{h}} = \frac{V}{2(2\pi)^2 v_{\mathrm{sl}}} \int_{\omega_{\min}}^{\omega_{\max}} \omega C(\omega) G''(\omega)\, \mathrm{d}\omega \ , \tag{3.4}$$

where V is the volume of the deformed rubber, C is the surface texture power spectral density which depends on the excitation frequency $\omega = qv_{\mathrm{sl}} = 2\pi v_{\mathrm{sl}}/\lambda$ and G'' is the frequency dependent shear loss modulus of the rubber.

In Fig. 3.5, a qualitative dependence of the resultant longitudinal friction force as a function of the excitation frequency is shown (for a constant temperature). A velocity (rolling or sliding) combined with a certain length scale (see Fig. 3.4) excites the tread rubber at a certain frequency and generates losses which depend on the viscoelastic properties of the tread rubber at this frequency (see Fig. 3.3). Rolling resistance result for lower excitation frequencies when the rolling velocity and the surface texture wavelengths on macro-scale and length scales of the contact patch interact. The contribution from hysteresis friction approximately lies within the frequency range of 10^2–10^6 Hz at a temperature of 20°C and becomes large for tread rubber sliding against macro and micro roughness with a velocity in the order of 1 m/s. The adhesive contribution is the highest when the ratio between the sliding velocity and a molecular length scale approximately equals the frequency for which the rubber dynamic properties exhibits the highest loss angle. This implies a very low sliding velocity in the order of 10^{-3} m/s in combination with force-oscillations on a molecular scale.

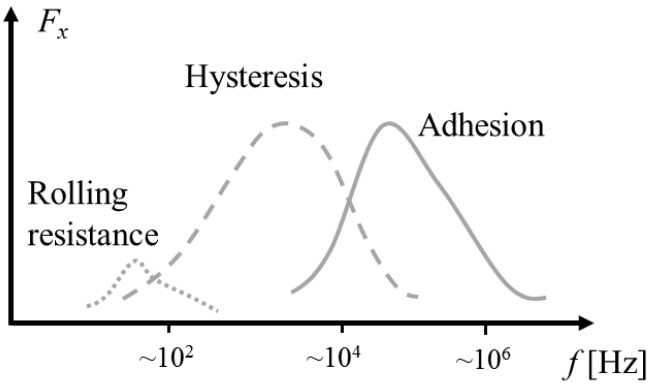

Figure 3.5: Principle character of separation of different contributions to the resultant longitudinal friction force as a function of frequency.

Activation of the different friction mechanisms is strongly dependent on the vehicle operating condition. For cruising at constant velocity, rolling resistance is activated which in turn demands for a counteracting adhesive force to maintain a constant velocity. For moderate acceleration or braking, a stronger adhesive force is generated due to a slightly larger sliding velocity. Heavy braking or acceleration lead to even higher sliding velocities in the tread–road contact which activates a combination of adhesive and hysteretic force generation with an increasing relative contribution from hysteresis friction as the sliding velocity increases. Very high sliding velocities lead to a temperature build up which shifts the region of maximum rubber hysteresis

to higher excitation frequencies [5]. However, the excitation frequency is not increased at the same rate, thus resulting in decreased hysteresis friction [28].

Chapter 4

Summary of appended papers

The contribution of the appended papers includes:

- Development of a computationally efficient approach to include the effect of small-scale roughness in a point force description for metal–metal rolling contacts (Paper A)
- Implementation of the proposed contact model (from Paper A) in a wheel–track interaction model for which prediction results are compared to field measurements (Paper B)
- Design of a unique test rig for detailed measurements of the rolling contact forces between a single tyre tread block and an interchangeable substrate (Paper C)
- In-depth knowledge of the contact forces and the friction coefficient of a single tyre tread block in rolling contact with asphalt (Paper D)
- Providing experimental results which show that the substrate roughness has significant influence on the friction coefficient of a tyre tread block in rolling contact (Paper E)

4.1 Paper A

A nonlinear state-dependent model for vibrations excited by roughness in rolling contacts

In the process of rolling, forces between the interacting structures excite vibrations which in turn lead to noise, wear and rolling resistance. The shape and roughness of the contacting surfaces lead to a nonlinear excitation process, which is therefore most accurately represented by time-domain models using full geometrical description of the contact. However, such models require complete sets of surface data and lead to high computational cost. To overcome these drawbacks, this paper proposes a state-dependent approach, in which the effect of contact stiffness as well as that from contact filtering (see Fig. 4.1) is included as dependent of vertical relative displacement (the state) in a point force expression. The advantages of the proposed modelling approach lies in its computational efficiency and in a large reduction of required surface data compared to models based on three-dimensional contact computations in each time step. The proposed methodology is applied to a steel ball in rolling contact with a steel beam, where two beams having different degrees of roughness are studied. Simulation results of the beam vibrations using the state-dependent approach are compared to results from both measurements and a fully linear model. To conclude, the state-dependent method proposed in this paper includes the influence of relative displacement in rolling contact simulations and moreover, it is proven functional for the investigated beam-ball interaction. With this, a useful tool is presented, which efficiently includes nonlinear effects due to varying relative displacement in rolling contacts.

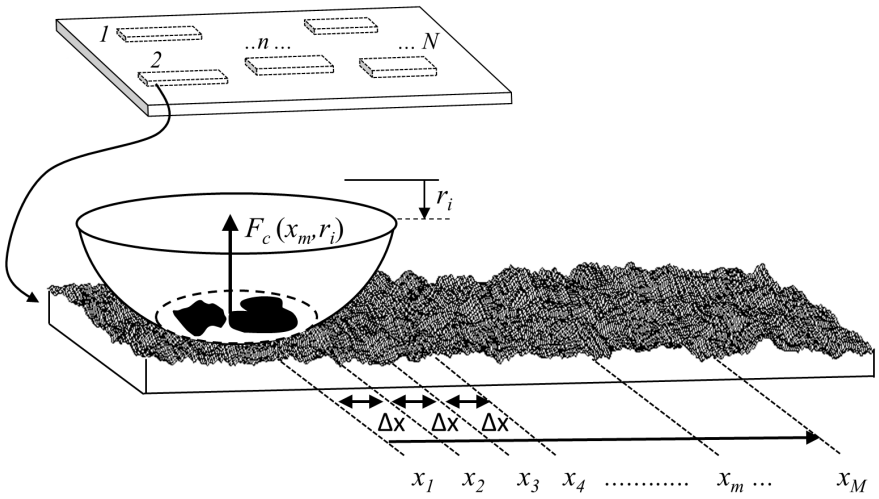

Figure 4.1: Schematic figure showing the use of detailed contact modelling to estimate the state-dependent contact filters [21].

4.2 Paper B

The influence of surface roughness on the contact stiffness and the contact filter effect in nonlinear wheel–track interaction

The contact model proposed in Paper A—which includes nonlinear contact stiffness and nonlinear contact filtering—is used to calculate contact forces and rail vibrations for wheel–track interaction. Green's functions for the linear dynamics of the wheel and the track are coupled with a point contact model, resulting in a computationally efficient description of the wheel–track interaction in time-domain (see Fig. 4.2). Numerical results are compared to field measurements of rail vibrations for passenger trains running at 200 km/h on a ballast track. As a result of a numerically based parametric analysis, only a small influence from contact nonlinearities induced by wheel and rail roughness is found. In addition, the nonlinear effects are found to be well approximated by the Hertzian contact stiffness and even with the linearised Hertzian stiffness for all the investigated cases but a combination of low pre-load and high roughness. Contact filtering nonlinearities where found to be significant for the higher investigated speed of 200 km/h and the combination of high roughness and low pre-load. In addition to the findings concerning nonlinear effects, the pre-calculated contact filters are observed to be strongly dependent on the character of the wheel and rail surface roughness. The lateral correlation of texture heights and the roughness magnitude in relation to the nominal wheel-rail relative displacement are parameters which possibly affect the character of contact filtering.

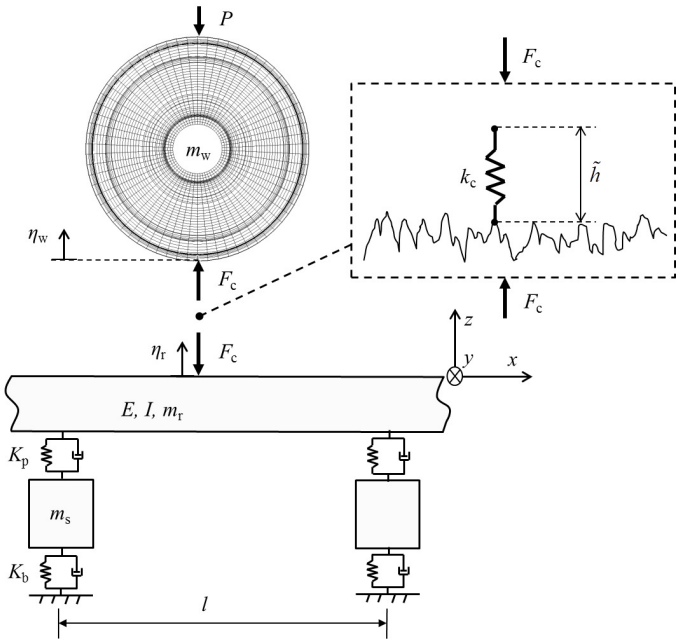

Figure 4.2: Overview of wheel-track interaction model [24].

4.3 Paper C

A compact internal drum test rig for measurements of rolling contact forces between a single tread block and a substrate

A test rig with a novel design referred to as a compact internal drum (CID) test rig (see Fig. 4.3) is developed for measurements of the three force components generated in the impact and release phase of a tyre tread block in rolling contact with a substrate. The test rig design provides realistic impact and release angles for the tread block–substrate contact and enables force measurements at high rolling speeds with a high signal-to-noise ratio. It is suitable for detailed investigations of the influence from rubber tread block and substrate characteristics since both the substrate as well as the sample tread block are fully interchangeable. The capability of the test rig to generate useful results is assessed by presenting results for both free rolling and accelerating condition at different rolling velocities and different static vertical pre-loads. The test rig thus provides results which contribute to the understanding of tyre–road interaction and can be used as input to modelling-based development of both tyres and roads aiming for improved handling, safety, energy efficiency and comfort.

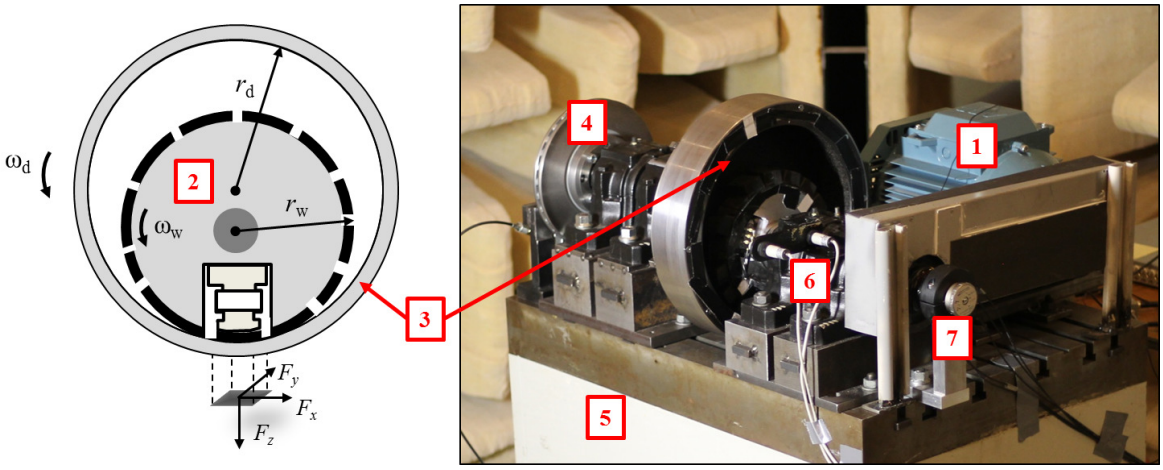

Figure 4.3: Overview of the test rig design with some of the components highlighted. An electric motor (1) generates torque on the solid wheel (2) which is covered by tread rubber on its circumference and is rolling against an interchangeable inner surface of a drum (3). An automotive disc brake (4) is used to brake the drum and create an accelerating torque for the solid wheel. A massive concrete block (5) gives alignment and inertia (dynamic stability) to the test rig. Optical sensors (6) are used to measure the rotational velocities of both the solid wheel and the drum. A slip ring assembly (7) is used to transfer the measured signals from the rotating solid wheel to a data acquisition system (adapted from [20]).

4.4 Paper D

Friction of a rubber tread block in rolling and sliding contact with asphalt—An experimental study

A detailed experimental study on the generation of rolling contact forces and the corresponding friction coefficient is performed using the CID test rig presented in Paper C. Measurements of the rolling contact between a truck tyre tread block and an asphalt substrate for different rolling velocities up to 60 km/h and different amount of slip ratios reveal substantial variations for the longitudinal force component and its corresponding friction coefficient. The longitudinal rolling contact forces are analysed by separately investigating the tread deformation and the rubber–substrate sliding which arise during rolling. To this end, measurements of the tread rubber dynamic stiffness as well as the friction of tread rubber in sliding contact with asphalt are performed (see Fig. 4.4). These characterisations are found to be useful since they provide approximate input values for an initial, promising attempt to separate the contributions from elastic deformation and sliding translation in the rolling contact. Conclusively, valuable insights are gained which has the potential to further reduce the gap between modelling of the fundamental physics of friction and empirically based knowledge for the most common rolling contact conditions.

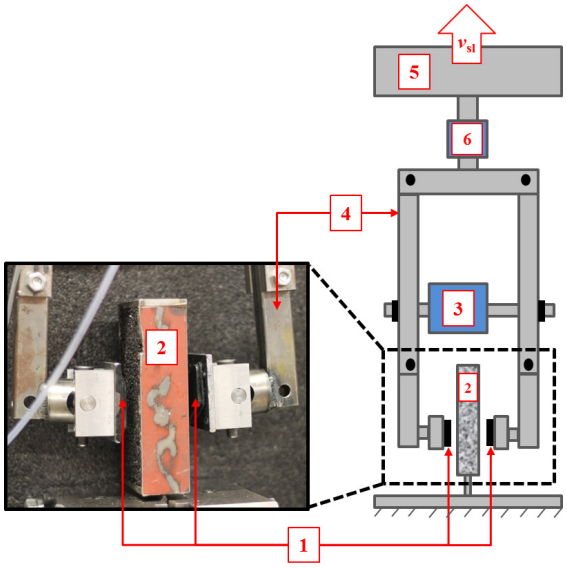

Figure 4.4: Schematic figure of the set-up used for characterisation of sliding friction. Two modified tread blocks (1) are pressed against an asphalt sample (2) using a pneumatic system (3); An aluminium structure (4) transmits the force to the upper column (5) via the force transducer (6). The test set-up is a temporary adaptation from its original design, aiming at the measurement of friction which arise in the manufacturing of composite structures [17] (figure from [23]).

4.5 Paper E

An experimental study on the influence of substrate roughness on the friction of a tread block in rolling and sliding contact

An experimental study of the friction coefficient is performed for a tyre tread block in rolling and sliding contact with two different asphalt substrates, a smooth aluminium substrate and an anti-slip tape substrate (see Fig. 4.5). The sliding friction coefficient is for all substrates seen to increase as the sliding velocity is increasing. However, the slope for the increasing friction as a function of sliding velocity differs significantly between the substrates, presumably due to differences in the respective contribution from adhesive and hysteresis friction mechanisms. Parametric studies of the rolling friction show that the choice of substrate as well as the rolling velocity and the slip ratio has significant influence on the resulting friction coefficient. A linear relation is found between the longitudinal rolling friction coefficient measured at low values of slip and the sliding friction coefficient measured at low sliding velocities. For the tests of rolling friction at higher values of slip, stick–slip conditions are observed for which the frequency content of the longitudinal force is seen to vary substantially between the different operating conditions and choice of substrate.

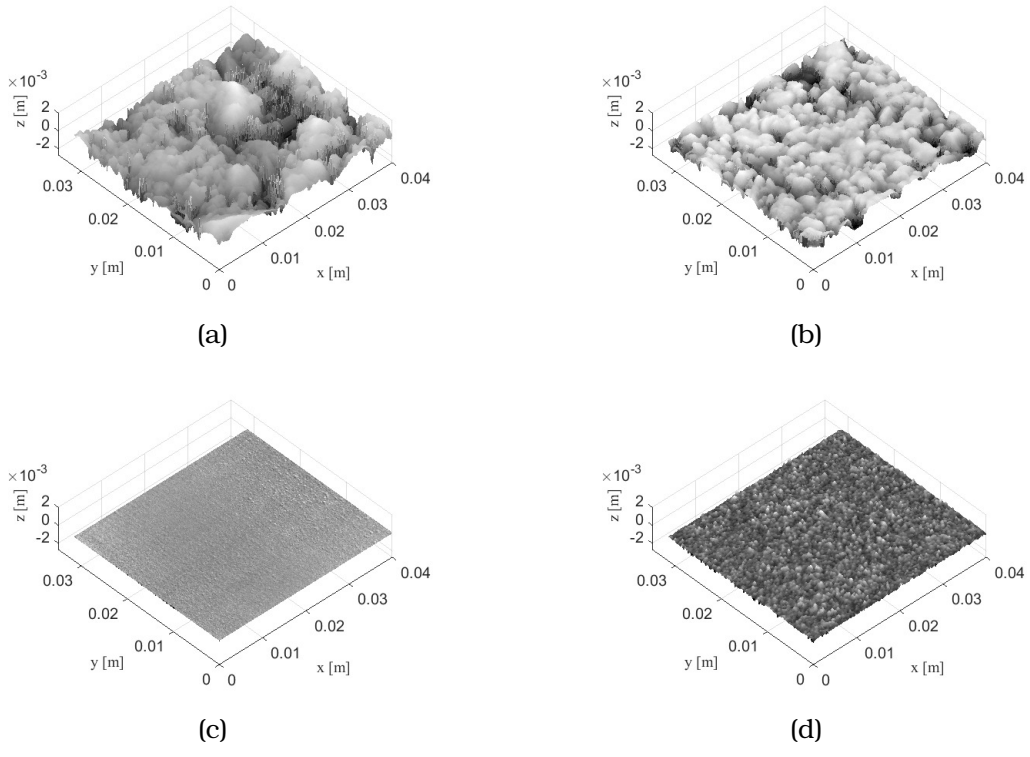

Figure 4.5: Surface texture heights for different substrates; a) asphalt with maximum stone size of 11 mm; b) asphalt with maximum stone size of 4 mm; c) aluminium; d) anti-slip tape substrate [22].

Chapter 5

Concluding remarks

Tyres and railway wheels as well as balls and rollers in bearings are examples of rolling elements which are crucial for efficient land transports and industrial applications. More stringent requirements on transportation and industry in terms of vibration and acoustic comfort, safety, wear and environmental impact lead to a constant need for improvements in the design of rolling contacts. Aspects such as rolling resistance (energy losses), durability (wear), comfort (vibration and noise) and the traction/braking performance are important, and they depend largely on the generation of forces in the rolling contact. However, it is still not fully understood how the surface roughness of the rolling element or the substrate influences this contact force generation. To this end, it is of interest to both industry and research institutes to develop modelling tools and experimental facilities which lead to increased knowledge in this subject.

Modelling of the vertical contact force generation in metal–metal rolling contacts is discussed in Paper A and Paper B. Since the shape and roughness of the contacting surfaces lead to a nonlinear vertical excitation process, it is most accurately represented by time-domain models using a full geometrical description of the contact. However, such models require complete sets of surface data which leads to a high computational cost. To overcome this drawback, a state-dependent approach is presented in Paper A, in which the contact stiffness and the contact filtering is included as dependent of vertical relative displacement (the state) in a point force expression. The advantages of the proposed modelling approach lies in its computational efficiency and in a large reduction of required surface data compared to models based on three-dimensional contact computations in each time step. The proposed method is subsequently implemented in a model for dynamic wheel–track interaction for which prediction results are presented and compared to field measurements of rail vibrations in Paper B. In addition, an extensive parametric study on the influence of contact nonlinearities on the

wheel–track interaction is presented therein. The influence of nonlinearities were found to be significant only for a high rolling speed and the combination of high roughness and low pre-load. An interesting output from the study is that the pre-calculated contact filters are observed to be strongly dependent on the character of the wheel and rail surface roughness. The lateral correlation of texture heights and the roughness magnitude in relation to the nominal wheel–rail relative displacement are parameters which possibly affect the character of contact filtering.

Experimental investigations of the tyre–road rolling contact forces are presented in Paper C, D and E. Due to the complicated mechanisms of rubber friction, which depend on the rubber viscoelasticity, the substrate roughness and the interfacial forces on a molecular length-scale, a complete physical description of the generation mechanisms of tyre–road friction is still lacking. Moreover, the modelling of interfacial details which determine the generation mechanisms require a high computational effort which further limits the development of reliable predictive tools for safer and more environmentally friendly tyre–road contacts. Experimental investigations are effective to increase the understanding of the friction force generation and possibly, they can lead to valuable input to modelling based research. However, a difficulty inherently lies in the measurement of contact forces within the contact patch, since any physical sensor which is applied to the contact patch will itself alter the contact conditions. Hence, the rolling contact forces are usually measured indirectly in the wheel hub which is unfortunate since the both the tyre and rim introduce dynamic contributions to the measured hub forces. These challenges are addressed in in Paper C, where the design of a novel compact internal drum test rig for measurements of the rolling contact forces which arise between a single tyre tread block and an interchangeable substrate is presented. Detailed three-axial force measurements are enabled by measurements close to the contact and by focusing primarily on the interfacial rubber–substrate contact, as the influence from tyre structural dynamics is left out. The test rig is used to measure the rolling contact forces between a truck tyre tread block and an asphalt substrate for different rolling velocities up to approximately 60 km/h and different amount of slip ratios, see Paper D. The results reveal substantial variations for the longitudinal force component and its corresponding friction coefficient. In addition, investigatory characterisations are performed for the dynamic viscoelastic deformation of the rubber and for the sliding friction of the rubber–asphalt contact which are found to be useful since they provide approximate input values for an initial, promising attempt to separate the contribution from elastic deformation and that from sliding friction. In Paper E, the influence of substrate roughness on the resulting rolling and sliding friction is investigated for two different asphalt surfaces, a smooth aluminium substrate and an anti-slip tape substrate. The magnitude of the

sliding friction coefficient measured at low sliding velocities is observed to be linearly correlated to the increasing slope of rolling friction as a function of the slip ratio (measured at low slip ratios). It is concluded that the choice of substrate, rolling velocity and amount of slip ratio has significant influence on the magnitude of the resulting rolling friction coefficient. These parameters are also seen to influence the occurrence of stick–slip conditions as well as its position of onset and the frequency content of the resulting oscillations.

Chapter 6

Suggestions for future work

The proposed state-dependent contact model is shown to be a useful tool which efficiently includes roughness-induced nonlinear effects in metal-metal rolling contacts. However, the investigated rolling contacts were limited to purely elastic contact deformations. Future work could therefore be focused on the inclusion of plastic and viscoelastic deformations, which would broaden the choice of materials to be investigated.

The viscoelastic properties of tread rubber are largely dependent on temperature. In order to monitor the temperature during measurements conducted with the CID test rig, a temperature sensor is embedded in the tread rubber. However, a proper investigation of the influence of temperature on the rolling contact forces and the corresponding friction coefficients remains and could be interesting to further investigate.

Bibliography

[1] famousscientists.org. web page, Nov. 2015.

[2] S. Björklund. *Elastic contacts between rough surfaces*. PhD thesis, KTH Royal Institute of Technology, Dpt. of Machine Design, 1995.

[3] J. Boussinesq. *Applications des potentials á l'etude de l'equilibre et du movement des solides elastique*. Gauthier-Villars, 1885.

[4] C. Gonzalez Diaz, P. Kindt, J Middelberg, S. Vercammen, C. Thiry, R. Close, and J. Leyssens. Dynamic behaviour of a rolling tyre: Experimental and numerical analyses. *Journal of Sound and Vibration*, 364:147–164, 2016.

[5] John D. Ferry. *Viscoelastic properties of polymers*. John Wiley & Sons, 1980.

[6] M. Fraggstedt. *Vibrations, damping and power dissipation in Car Tyres*. PhD thesis, KTH - Royal Institute of Technology, Dpt. of Aeronautical and Vehicle Engineering, 2008.

[7] Martin Gießler. *Mechanismen der Kraftübertragung des Reifens auf Schnee und Eis*. PhD thesis, Karlsruhe Institut für Technologie (KIT), 2011.

[8] R. Gnadler, H-J. Unrau, H. Fischlein, and M. Frey. Ermittlung von μ - schlupf-kurven an pkw-reifen. Technical report, Forschungsvereinigung Automobiltechnik e.V. (FAT), 1995.

[9] J. A. Greenwood and J. B. P. Williamson. Contact of nominally flat surfaces. *Proceedings of the Royal Society of London A*, 295:300–319, 1966.

[10] K. A. Grosch. The relation between the friction and visco-elastic properties of rubber. *Nature*, 197:858, 1963.

[11] Johannes Gültlinger. *Kraftübertragung und Fahrbahn-verschleiß durch Spikereifen*. PhD thesis, Karlsruher Institut für Technologie, 2015.

[12] G. Heinrich and M. Klüppel. Rubber friction, tread deformation and tire traction. *Wear*, 265:1052–1060, 2008.

[13] H. Hertz. Über die berührung fester elastischer körper (on the contact of rigid elastic solids). *Journal für die reine und angewandte Mathematik*, 1882.

[14] IEA. Energy technology perspectives - pathways to a clean energy system. Presentation slides, 2012.

[15] K. L. Johnson. *Contact mechanics*. Press syndicate of the university of Cambridge, 1985.

[16] Frank Klempau. *Untersuchungen zum Aufbau eines Reibwertvorhersagesystems im fahrenden Fahrzeug*. PhD thesis, Technischen Universität Darmstadt, 2003.

[17] Y. R. Larberg and M. Åkermo. On the interply friction of different generations of carbon/epoxy prepreg systems. *Composites: Part A*, 42:1067–1074, 2011.

[18] F. Liu, M. P. F. Sutcliffe, and W. R. Graham. Prediction of tread block forces for a free-rolling tyre in contact with a smooth road. *Wear*, 269:672–683, 2010.

[19] I. Lopez, R. E. A. Blom, N. B. Roozen, and H. Nijmeijer. Modelling vibrations on deformed rolling tyres—a modal approach. *Journal of Sound and Vibration*, 307:481–494, 2007.

[20] O. E. Lundberg, I. Lopez Arteaga, and L. Kari. A compact internal drum test rig for measurements of rolling contact forces between a single tread block and a substrate. *Submitted to Measurement*, 2016.

[21] O. E. Lundberg, S. Finnveden, S. Björklund, M. Pärssinen, and I. Lopez Arteaga. A nonlinear state-dependent model for vibrations excited by roughness in rolling contacts. *Journal of Sound and Vibration*, 345:197–213, 2015.

[22] O. E. Lundberg, L. Kari, and I. Lopez Arteaga. An experimental study on the influence of substrate roughness on the friction of a tread block in rolling and sliding contact. *To be submitted*, 2016.

[23] O. E. Lundberg, L. Kari, and I. Lopez Arteaga. Friction of a tread block in rolling and sliding contact with asphalt—an experimental study. *Submitted to Wear*, 2016.

[24] O. E. Lundberg, A. Nordborg, and I. Lopez Arteaga. The influence of surface roughness on the contact stiffness and the contact filter effect in nonlinear wheel-track interaction. *Journal of Sound and Vibration*, 366:429–446, 2016.

[25] M. Mokhtari, D. J. Schipper, and T. V. Tolpekina. On the friction of carbon black- and silica-reinforced br and s-sbr elastomers. *Tribology Letters*, 54:297–308, 2014.

[26] D. F. Moore. *The Friction of Pneumatic Tyres*. Elsevier, 1975.

[27] D. J. O'Boy and A. P. Dowling. Tyre/road interaction noise—a 3d viscoelastic multilayer model of a tyre belt. *Journal of Sound and Vibration*, 322:829–850, 2009.

[28] B. N. J. Persson. Rubber friction: role of the flash temperature. *Journal of physics: Condensed matter*, 18:7789–7823, 2006.

[29] A. Schallamach. A theory of dynamic rubber friction. *Wear*, 6:375–382, 1963.

[30] Robert Thomson. Improvement in carriage-wheels (us patent), 1847.

[31] K. Vorvolakos and M. Chaudhury. The effects of molecular weight and temperature on the kinetic friction of silicone rubbers. *Langmuir*, 19:6778–6787, 2003.

[32] Chunyang Xie. *Experimentelle Untersuchungen zur Interaktion zwischen Pkw-Reifen und Fahrbahn beim Bremsen*. PhD thesis, Technischen Universität Darmstadt, 2001.

Part II

Appended Papers